25/1-24-84 ∂s (1) IV-16001

SANDIA REPORT SAND84–0638 • Unlimited Release • UC–13
Printed May 1984

SAND--84-0638

DE84 014821

Magnetic Induction System for Two-Stage Gun Projectile Velocity Measurements

R. L. Moody, C. H. Konrad

Prepared by
Sandia National Laboratories
Albuquerque, New Mexico 87185 and Livermore, California 94550
for the United States Department of Energy
under Contract DE-AC04-76DP00789

MASTER

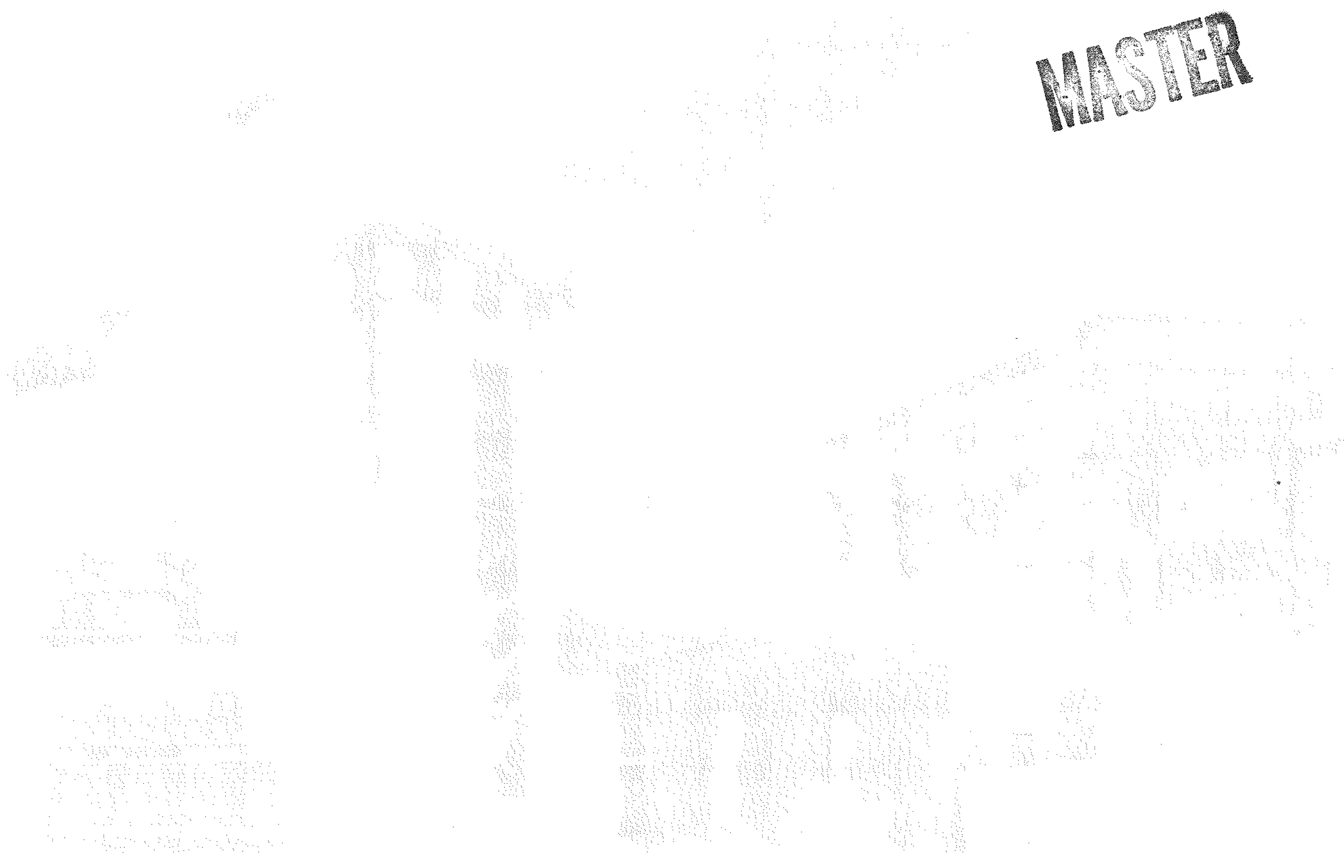

DISTRIBUTION OF THIS DOCUMENT IS UNLIMITED

SF2900Q(8-81)

Printed in the United States of America
Available from
National Technical Information Service
U.S. Department of Commerce
5285 Port Royal Road
Springfield, VA 22161

NTIS price codes
Printed copy: A100
Microfiche copy: A01

DISCLAIMER

DISCLAIMER

Distribution
Category UC-13

SAND84-0638
Unlimited Release
Printed May 1984

Magnetic Induction System for Two-Stage Gun Projectile Velocity Measurements

R. L. Moody and C. H. Konrad
Thermomechanical & Physical Division 1534
Sandia National Laboratories
Albuquerque, New Mexico 87185

ABSTRACT

A magnetic induction technique for measuring projectile velocities has been implemented on Sandia's two-stage light gas gun. The system has been designed to allow for projectile velocity measurements to an accuracy of $\sim$ 0.2 percent. The velocity system has been successfully tested in a velocity range of 3.5 km/s to 6.5 km/s.

Contents

Figures

1 Introduction

The purpose of developing a new velocity system for the two-stage light gas gun is to provide an accurate and reliable technique for measuring projectile velocities. To meet this objective, it is necessary to replace the coaxial pins which are presently used. Coaxial pins are generally not accurate for two-stage gun applications, due to the small transit time over which the time-interval measurements can be made. Uncertainties arising from tilt and pin gaps become a significant fraction of the transit time, increasing the errors in velocity measurements. In addition, blow-by preceding the projectile can also pre-trigger the coaxial pins, reducing reliability. Both of these limitations can be overcome by replacing the coaxial pins with a velocity measuring system utilizing a magnetic induction technique. An adaptation of a similar system, that is currently in use at Los Alamos National Laboratory, has been implemented,[1] and is discussed in this paper.

In the following sections, the design and operation of the magnetic induction system is described. Typical records obtained over a range of velocities are included along with a discussion of errors (including the procedure that is involved in achieving measurements to an accuracy of $\sim$ 0.2 percent).

2 Physical Set-Up of the Magnetic Velocity Induction System

There are three considerations to the physical set-up of the Magnetic Velocity Induction System (MAVIS). First, the technical basis for MAVIS is described. Second, the procedure for integrating MAVIS with the two-stage catcher tank and target-holder assembly is discussed. Third, the alignment of the entire system prior to actual testing is discussed. These topics will be addressed in the order listed.

From Figures 1 and 2, it can be seen that MAVIS consists of several separate parts. We will discuss the magnets first. They are Ceramic-5 permanent magnets obtained from Permag, Inc. Torroidal in shape, the magnets have a residual flux density of 3,800 gauss, and a coercive force of 2,400. Nylon forms the cylindrical base upon which all the system pieces are mounted. Tolerances are held to $\pm$.025 mm on all dimensions and are closely inspected prior to assembly to ensure accurate coil and magnet spacing. Total system accuracy is discussed later in this report.

The coils consist of six turns of AWG #32 coated copper wire. All coils are wound in the same direction, and connected according to the circuit diagram shown in Figure 3. A 250 pF capacitor is connected across each of the coil outputs for noise reduction; a 51 ohm resistor on the output side of the coil is necessary for impedance matching.

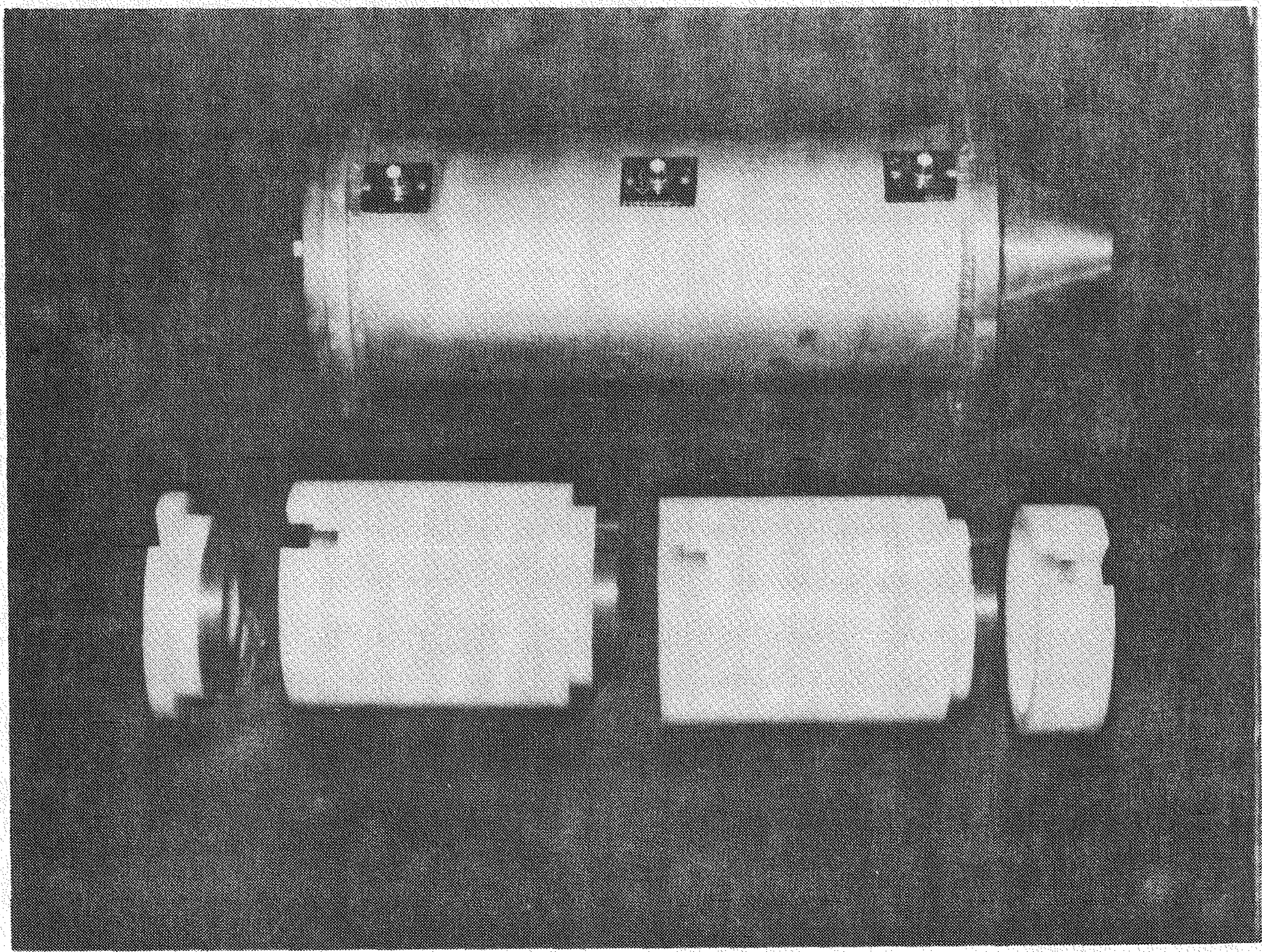

Figure 1. MAVIS

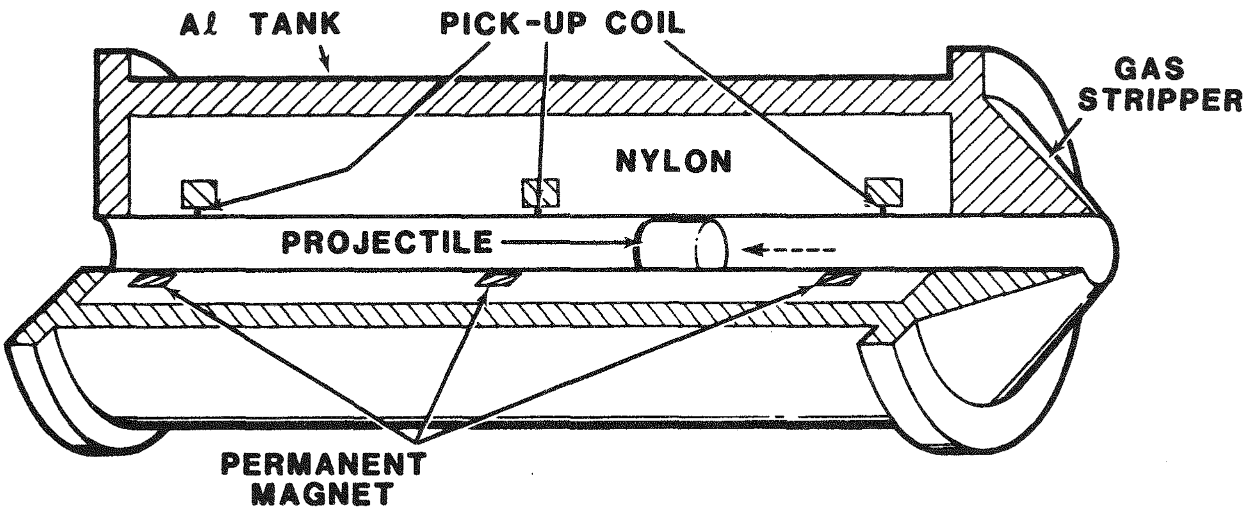

Figure 2. Cutaway View of MAVIS

An aluminum cylinder is used to confine the coils, magnets, circuits, and nylon base assembly; and also for mounting the system into the two-stage catcher tank. Concentricity of all parts is held to ± .025 mm. A gas stripper is installed at the muzzle-facing end of the cylinder. Though it does not prevent gases from flowing through MAVIS, it does divert most of the excess gases away from the target and instrumentation. BNC bulkhead connectors are currently used in MAVIS, but others may be adapted.

As shown in Figure 4, MAVIS is mounted within the two-stage catcher tank. Concentricity of MAVIS with the bore of the gun is the prime concern in mounting. The target assembly is located approximately 175 mm behind MAVIS. Direct mounting of the target to MAVIS was attempted at first, but proved to be highly detrimental, due to the effects of shock coupling from the target to MAVIS.

In this section, the alignment of MAVIS concentric to the bore of the two-stage gun is discussed. Using a small HeNe laser mounted in a four-axis translation mount, the beam is first aligned to be concentric and coaxial with the bore of the launch tube. After achieving this, the beam is "fine-tuned" to the launch tube bore axis by inserting a small lexan cylinder plug, with a .250 mm hole on its axis into the breech end of the launch tube. Following alignment of the laser beam to this plug, a similar plug is inserted into the muzzle end of the launch tube, providing a small diameter (2 mm) beam in the catcher tank. A plug with a 2 mm center hole is inserted into the gas stripper end of MAVIS. Adjustments are made to the mounting assembly to which the system is attached until the beam is concentric and coaxial with the center hole of the plug. Next, a similar plug is inserted into the back end of MAVIS and using a three-point hex-bolt ring, the MAVIS housing is adjusted to bring the beam concentric and coaxial through the center hole of the rear plug. This assures that the axis of MAVIS and the axis of the launch tube are colinear.

Tilt alignment of the target assembly is performed after the concentric and coaxial alignment procedures have been completed. An optically flat Dynasil 1000 fused silica sample with a spectral mirror scribed with center cross hairs is mounted in a target plate, which is then attached to the target holding assembly. The alignment plugs from both ends of MAVIS are then removed, providing more light for a larger centering X on the cross hairs. First, the target mirror assembly is mounted so that the laser beam is at the center of the cross hairs; tilt adjustment screws of the target mount are then used to adjust the mirror to reflect a cross-hatch pattern centered on the face of the muzzle plug. This assures coaxial alignment of the reflected beam with respect to the incoming beam. When the cross-hatch pattern is sufficiently centered on the muzzle plug, that plug is removed along with the breech end plug. The same procedure for centering the cross-hatch pattern is repeated at the face of the laser tube (using a 3x5 card with a 2 mm hole held in front of the laser). Usually, only a minor adjustment is necessary for centering. Both the primary and reflected beams are now colinear with the axis of MAVIS and the axis of the launch tube. Nominal tilt using this method is 10 milliradians or less. Repetition of the above procedures is necessary after each test to ensure coaxial alignment of MAVIS, the launch tube and center of the target.

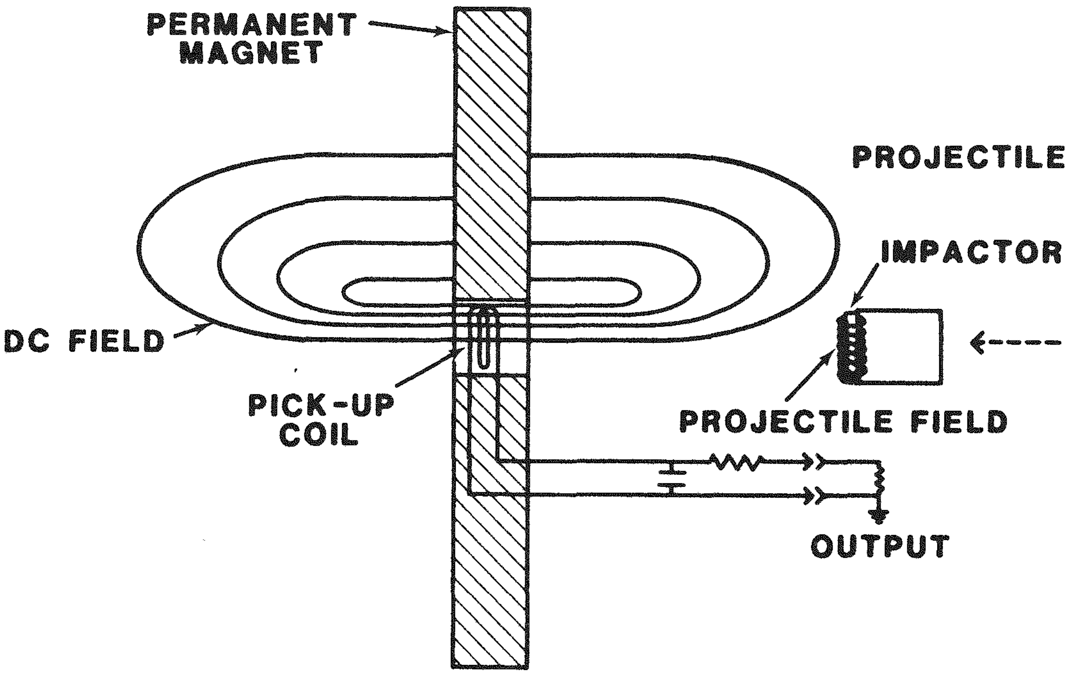

Figure 3. MAVIS Circuitry and Magnetic Fields

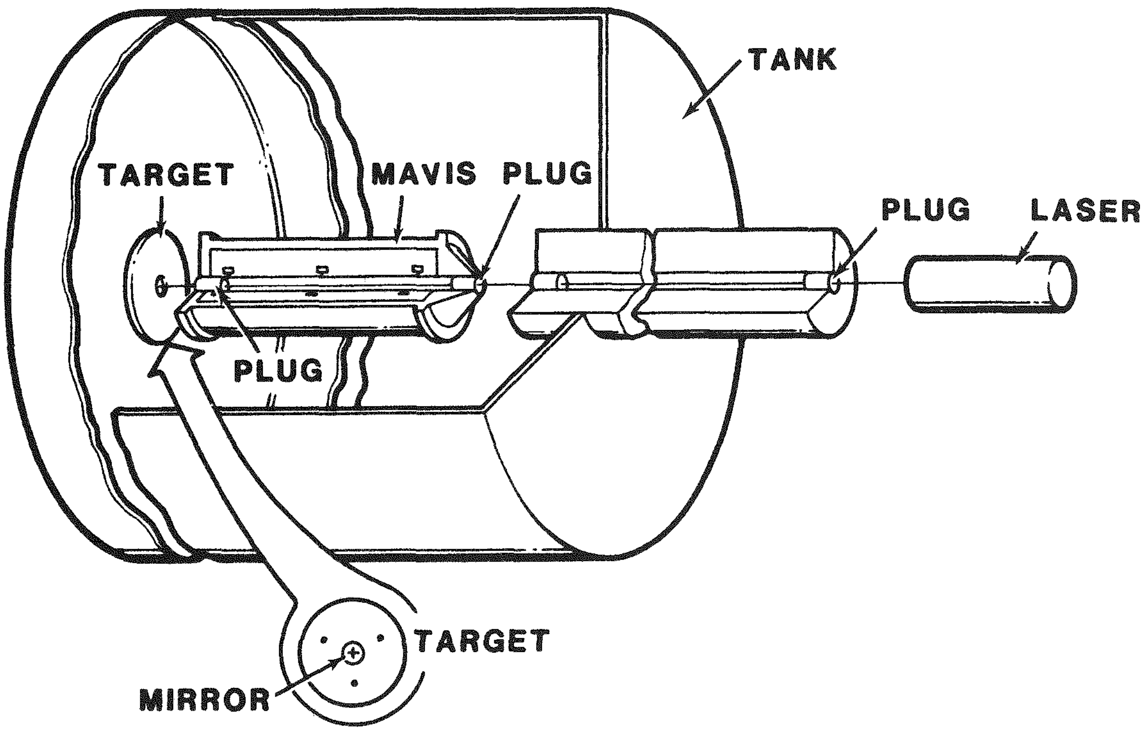

Figure 4. Alignment of MAVIS

Currently, oscilloscope records and time-interval counters are used to measure the time interval between the coils, and thus projectile velocity. Typical output from the coils is about 3-6 volts depending upon projectile velocity. Sweep speeds are set, based upon expected projectile velocity, with allowance for approximately 10% variation in projected velocity. A positive or negative trigger mode is determined by the north-south orientation of the magnets and the direction of the coil windings. Calibration time marks are pre-photographed prior to the shot to compensate for nonlinearity of the scope horizontal time base. After the test, measurements are taken at or near the zero (DC level) crossover points of the oscilloscope records to obtain the time interval needed to calculate the velocity.

A more direct method involves the use of time-interval counters. Here, a direct reading is taken from the indicated time interval, and a velocity is calculated. Nominal trigger levels for the time interval counters are 0.3 to 1 volt in magnitude. No difference in velocity has been observed in this 0.3 to 1 volt range providing the start and stop voltage levels are identical.

3 Theory of Operation

Eddy currents are induced in the metallic impactor as the projectile enters the field of the permanent magnet as indicated in Figure 3. The currents flowing in the impactor set up their own magnetic field which interacts with the field of the permanent magnet. A current is therefore induced in the stationary pick-up coil due to the approaching impactor field.[2] Figure 5 shows a typical output signal from the three coils. When the impactor approaches the pick-up coil, the coil current and therefore the voltage displayed on the oscilloscopes increases in the positive direction. The polarity of these signals is arbitrary in the sense that it depends upon the direction in which the magnets were installed.

Induced currents in the pick-up coil continue to increase until the center of the impactor field is centered in the coil. At this time, the impactor field is crossing the pick-up coil winding at a constant rate; therefore, the flux change drops to zero. When the above sequence is completed, the induced field of the pick-up coil collapses trying to maintain its current, thus driving the output signal rapidly in the negative direction. As the pick-up coil output crosses the zero voltage point, the impactor field and hence the impactor is centered in the coil. As the impactor passes the coil, its field will again cut the pick-up coil windings, but in the opposite direction and with diminishing field strength. This drives the pick-up coil output to its maximum negative excursion. As the impactor exits the field of the permanent magnet and its distance from the pick-up coil increases, the coil output decreases to zero. This process is repeated with each of the three magnet/pick-up coil stations.

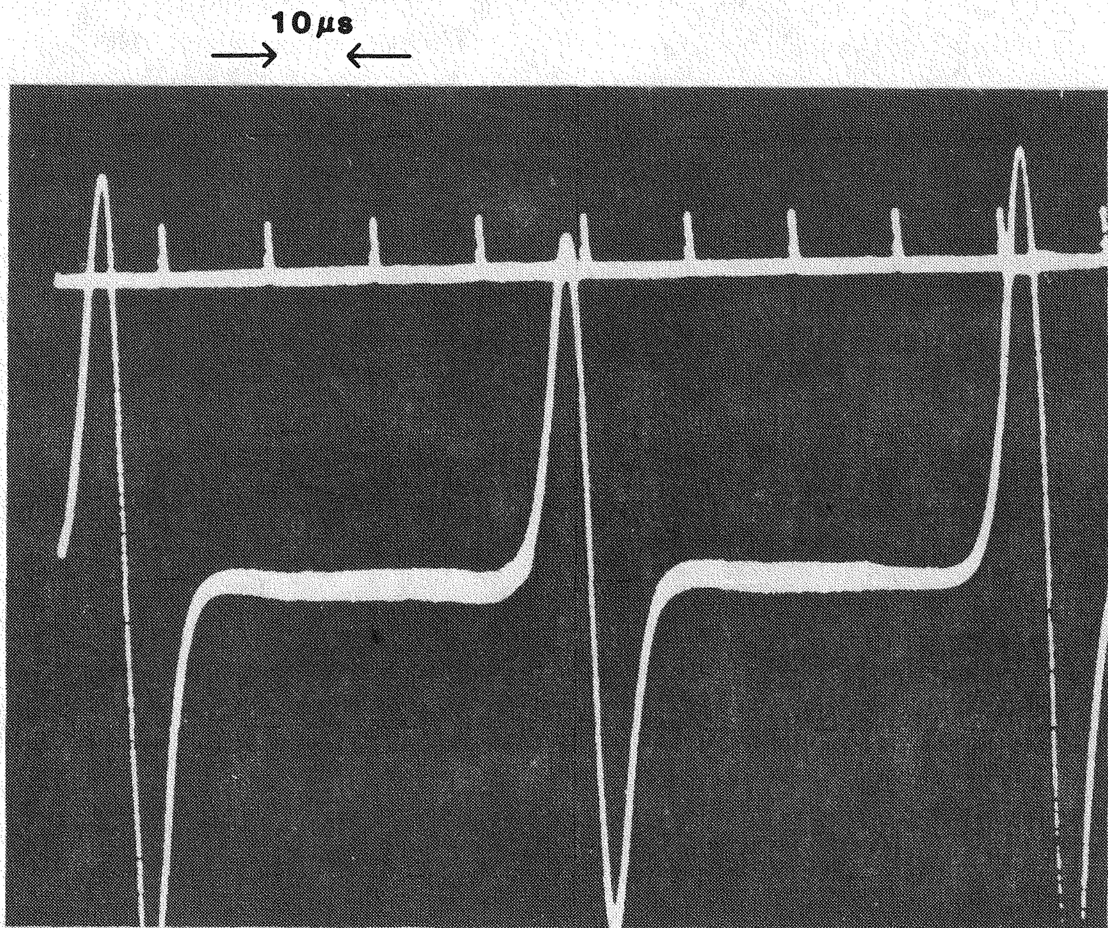

Figure 5. Typical MAVIS Output Signals

4 Error Analysis

There are several inherent error components within MAVIS. Probable sources of error are physical measurement of coil position, thermal expansion of the nylon components, change in magnet or coil position with use, and voltage settings of the time-interval counters.

Coil position is known to within $\pm$ 0.05 mm prior to assembly, and has subsequently been rechecked after use without indication of change. Using the shortest distance between coils of 152.4 mm, a 0.05 mm measurement error produces a $\pm$ 0.03% error in velocity.

It is not possible for the magnets or the coils to change position without serious and obvious damage to MAVIS. Either visible physical damage or deformation of the oscilloscope record waveform will indicate such a position change. The magnets may fracture after some time; a problem which will usually be indicated by a reduction in oscilloscope record voltage amplitudes, as shown in the middle waveform in Figure 5. This will be a source of error as it will change the slope of the cross over. A single crack will not cause this effect; the magnet must be considerably fragmented to effect an amplitude change. This problem necessitates a change in magnets to correct the error.

Using the quoted units for linear thermal expansion[3] of nylon (pure 66) of 83×10^{-6}/C gives a probable error of 0.04% with a $\pm$ 5°C temperature change. However, the probability of a $\pm$ 5°C change in temperature in an environmentally controlled building is unlikely; thus, this is a maximum expected error. A final argument against this error is the use of Nylatron GS versus nylon. Nylatron GS has a far lower coefficent of thermal expansion (Nylatron GS, 9 x 10^{-6}/C).[4] All future MAVIS systems will be constructed from Nylatron GS material.

Time-interval counter voltage settings give the greatest single source of probable error. As can be seen from Figure 5, the slope from peak to peak may cover a time interval of approximately 80-200 nanoseconds depending upon projectile velocity. The trigger level voltage settings are set to start and stop the counter near the zero crossing point (i.e. -0.3 volts). Due to the voltage slope of the signal (200 ns/volts slope) the counter trigger level settings are very important. If the input levels are set at $\pm$ 100 mv around the desired 0.3 volt point and assuming a peak to peak amplitude of 6 volts which is nominal for a 4.5 km/s projectile velocity, the error associated with the trigger level would be $\simeq$ 40 ns error over 152.4 mm distance. Over the 152.4 mm distance or 33.9 μs time interval, a 40 ns reading error would yield a 0.12% error in velocity. Of course, this error drops by a factor of 2 over the 304.8 mm reading, to $\simeq$ 0.06%.

Totaling these errors we have 0.04% from thermal changes, 0.03% from coil to coil measurement errors, and 0.12% from trigger voltage levels; giving 0.19% as a maximum error for interval measurements over 152.4 mm. A total over a 304.8 mm distance would approach $\simeq$ 0.13% error. With no temperature change and accurate setting of trigger levels, even lower errors should result.

5 Acknowledgments

The authors wish to thank Dennis Shampine of Los Alamos National Laboratory for suggesting the technique, and Robert Hardy of Sandia National Laboratories for his help in designing and building all fixtures necessary to adapt the system to the STAR Facility Two-Stage Light Gas Gun. Special thanks go to Dennis Grady and Larry Bacon of Sandia National Laboratories for their theoretical assistance, and to L. C. Chhabildas for his assistance in guiding the organization of this paper.

6 References

1. Conversations with Dennis Shampine, Los Alamos National Laboratory.
2. Conversations with Larry Bacon, 1232, Sandia National Laboratories.
3. J. Brandrup and E. H. Immergut, *Polymer Handbook*, Second Edition, J. Wiley (1975).
4. *Manufacture Literature*, Polymer Corporation, Reading, PA.

DISTRIBUTION:

Ben Barrett
GM/DRL Delco Electronics SBO
6767 Hollister Avenue
Goleta, CA 93117

Henri Bernier
Commissariat a l'Energie Atomique
Centre d'Etudes de Limeil - BP 27
94190 Villenueve Saint Georges
FRANCE

Stephen Bless
University of Dayton Research Institute
300 College Park Avenue
Dayton, OH 45469

George Burghart
Science Applications, Inc.
201 West Dyer Road, Unit B
Santa Ana, CA 92707

John Burnett
General Electric Company
Armament & Electrical Systems
Lakeside Avenue
Burlington, VT 05402

John Cable
ARVIN/CALSPAN Field Service Inc.
von Karman Gas Dynamics Facility
Arnold Engineering
Arnold AFB, TN 37389

J. A. Charest
DYNASEN, Inc.
20 Dean Arnold Place
Goleta, CA 93107

Herb Curchack
ERADCOM, Harry Diamond Labs
2800 Power Mill Road
Adelphi, MD 20783

J. Dumas
Laboratoire de Recherches
Balistiques et Aerodynamiques
27207 Vernon, B.P. 914
FRANCE

J. W. Evans
USA Ballistic Research Laboratory
Aberdeen Proving Ground, MD 21005

John A. Fitzgerald
Honeywell Proving Ground
23100 Sugar Bush Road
Elk River, MN 55330

Nilson Froula
Corrales Applied Physics Co.
1005 South Star Route
Corrales, NM 87048

P. W. W. Fuller
Royal Armament Research and
Development Establishment
Ballistics Branch R31
Ft. Halstead, Sevenoaks
Kent, ENGLAND

M. Giraud
Institut Franco-Allemand
de Recherches de Saint-Louis
12, rue de l'Industrie
68301 Saint-Louis FRANCE

Bill Holt
Naval Surface Weapons Center
Dalgren, VA 22448

Charles Honodel
Lawrence Livermore National Laboratory
P. O. Box 808, L-368
Livermore, CA 94550

Hidetaka Ichikawa
Mitsubishi Heavy Industries
3000 Tana Sagamihara-shi
Kanagawaken 229 JAPAN

Dr. E. Igenbergs
Institut fuer Luft and Raumfahrt
Technische Universitaet
8000 Muenchen 2
Arcisstrasse 21
Federal Republic of Germany

Peter Intrieri
NASA/Ames Research Center
Moffett Field, CA 94035

William Isbell
Effects Technology, Inc.
5385 Hollister Avenue
Santa Barbara, CA 93111

W. J. Kolkert
Prins Maurits Laboratory
TNO P. O. Box 45
2280 AA Rijswijk
The Netherlands

Dan Krupovage
U. S. Air Force
6886th Test Group
Test Track Division
Holloman AFB, NM 88330

K. F. Leisinger
Dir. Dipl-Ing. H. Schulte
ERP St. 91 d. Bw
4470 Meppen
Federal Republic of Germany

David Lippy
Martin-Marietta Corporation
P. O. Box 5837
Orlando, FL 32855

J. Martineau
Centre de Vaujours
Boite Postale 7
93270 Sevran FRANCE

W. L. McKay
AVCO Systems Division
201 Lowell Street
Wilmington, MA 01887

Lewis Moir
Defense Research Establishment
P. O. Box 8800
Courcelette P.Q. Canada GIV 3K6

Sven Nordstrom
FMV-F:AP/FOA 276
S-546 01 Karlsborg
National Defense Research Institute
Linnegatan 89, Stockholm
S-104 50 Stockholm, SWEDEN

Akira Sawaoka
Tokyo Institute of Technology
Research Lab. Eng. Matls.
4259 Nagatsuta, Midori
Yokohama 227, JAPAN

Alois Stilp
Ernst-Mach-Institut der
Fraunhofer-Gesellschaft
Eckerstrasse 4
D 7800 Freiburg i. Br.
Federal Republic of Germany

Jacques Vermorel
Institut Franco-Allemand de
Recherches de Saint-Louis
12, rue de l'Industrie
68301 Saint-Louis FRANCE

Ed Webster
Department of the Army
ARRADCOM Test Site
Fort Dix, NJ 08640

Alex B. Wenzel
Southwest Research Institute
6220 Culebra Road
San Antonio, TX 78284

Andrew E. Williams
Code 7945
U.S. Naval Research Laboratory
Washington, DC 20375

G. L. Winchenbach
Air Force Armament Laboratory
Elgin AFB, FL 32542

Toshiro Yamada
Department of Mech. Engineering
Kyoto University
Sakyo-Ku, Kyoto 606 JAPAN

Sandia Internal:

1130 G. A. Samara
1131 B. Morosin
1131 M. B. Boslough
1131 R. A. Graham
1131 R. E. Setchell
2513 J. E. Kennedy
2513 S. A. Sheffield
2513 P. L. Stanton
2514 B. H. Van Domelen
2531 W. D. Williams
2532 J. J. Marron
1510 J. W. Nunziato
1520 D. J. McCloskey
1530 L. W. Davison
1534 J. R. Asay
1534 L. M. Barker
1534 L. C. Chhabildas
1534 D. E. Cox
1534 D. E. Grady
1534 R. D. Hardy
1534 C. H. Konrad (5)
1534 R. L. Moody (25)
1534 J. M. Miller
1534 D. D. Scott
1534 J. L. Wise
1540 W. C. Luth
Attn: 1542 B. M. Butcher
3141 C. M. Ostrander (5)
3151 W. L. Garner (3)
3154-4 C. Dalin (25)
For DOE/TIC